J_2 INVARIANT RELATIVE ORBITS FOR SPACECRAFT FORMATIONS

HANSPETER SCHAUB and KYLE T. ALFRIEND
Department of Aerospace Engineering, Texas A&M University, College Station, TX 77843-3141, U.S.A.

(Received: 7 July 1999; accepted: 28 November 2000)

Abstract. An analytic method is presented to establish J_2 invariant relative orbits. Working with mean orbit elements, the secular drift of the longitude of the ascending node and the sum of the argument of perigee and mean anomaly are set equal between two neighboring orbits. By having both orbits drift at equal angular rates on the average, they will not separate over time due to the J_2 influence. Two first order conditions are established between the differences in momenta elements (semi-major axis, eccentricity and inclination angle) that guarantee that the drift rates of two neighboring orbits are equal on the average. Differences in the longitude of the ascending node, argument of perigee and initial mean anomaly can be set at will, as long as they are setup in mean element space. For near polar orbits, enforcing both momenta element constraints may result in impractically large relative orbits. It this case it is shown that dropping the equal ascending node rate requirement still avoids considerable relative orbit drift and provides substantial fuel savings.

Key words: Spacecraft Formation Flying, J_2 invariant relative orbit, analytic methods, satellite theory

1. Introduction

Previous studies on the relative motion of spacecraft in Earth orbit have typically used the Clohessy–Wiltshire (CW) equations [3, 5, 7, 8] to describe the relative equations of motion. With these linearized equations periodic motions in the relative motion reference frame have been identified. These periodic motions include in-plane, out-of-plane, and combinations of these two motion types. When one includes perturbations, some of these periodic orbits are no longer achievable without control to overcome the deviations. A simple example demonstrates this fact. Consider an out-of-plane relative motion caused by a difference in inclination angles. Due to the J_2 perturbation, the inclination difference will cause a differential nodal precession rate between the two satellites resulting in an oscillatory out-of-plane motion with increasing amplitude. However, the linear CW equations do not show this motion; they indicate an out-of-plane oscillatory motion with a constant amplitude. To maintain a relative orbit designed with the CW equations, periodic orbit corrections are necessary to cancel deviations caused by the J_2 perturbations. Further, a reference motion and the accompanying state transition matrix might result in an out-of-plane control that changes inclination because the state transition matrix does not indicate the increasing amplitude caused by the inclination difference. For these reasons it is necessary for the reference motion to

Celestial Mechanics and Dynamical Astronomy **79:** 77–95, 2001.

include at least the J_2 gravitational perturbation effect. The satellites considered are assumed to be equal in size and shape. Therefore, compared to the J_2 effect, the differential drag effect is of lesser importance in this study and is neglected. Note that referring to two neighboring orbits as being J_2-invariant implies in this paper that the angular drift rates of the longitude of the ascending node and the mean latitude angle are equal on the average. This statement does not guarantee that the distance between two spacecrafts will remain small. Since the argument of perigee and the mean anomaly of each spacecraft may drift at different rates, it is possible for the lines of perigee to move apart over time. As this happens, the relative orbit geometry will either expand or contract. Control strategies to re-establish proper argument of perigee separation are being investigated separately and are not discussed in this paper. Note, however, that the differential drift rate in the argument of perigee is typically rather slow. Using the conditions derived in this paper, the relative orbit geometry will appear fixed for dozens of orbits.

The relative orbit geometry between two neighboring satellites is described using the differences in *mean orbit elements*. Mean orbit elements are used because the three mean momenta are constant and the three angles vary linearly with time, whereas all six osculating elements vary with time. Since the mean Hamiltonian is a function of only the momenta, the relative rates between the two bodies are defined by the differences in the three momenta. Thus, the selection of initial conditions to match the average drift rates is reduced from a six-dimensional space to a three-dimensional space. Brouwer's artificial satellite theory without drag [2] is used to search for J_2 invariant relative orbits. In particular, we seek to match the average drift rates of the two neighboring orbits up to first order, resulting in a closed-path relative motion that is practically invariant to the J_2 perturbations. The advantage of these relative orbits is that they will need very little control to cancel the J_2 effects, and thus require less fuel to maintain.

2. Problem Statement

At any instant of time, the current inertial position and velocity vectors can be transformed into corresponding instantaneous orbit elements. In the absence of perturbations, these elements are constants. Adding the J_2 perturbation causes the elements to vary according to three types of motion, namely secular drift, short period motion and long period motion. The long period term is the period of the apsidal rotation. Over a short time this looks like a secular growth of order J_2^2. The short period growth manifests itself as oscillations of the orbit elements, but does not cause the orbits to drift apart. The relative secular growth is the type of growth that needs to be avoided for relative orbits to be J_2 invariant. This growth is best described through *mean orbit elements*. These are orbit averaged elements which do not show any of the short period oscillations. Mean elements can be obtained analytically or numerically. Highly accurate mean elements that must in-

clude atmospheric drag, tesseral harmonic and third body effects probably require numerical averaging. In this paper we use an analytical approach to help determine the accuracy that will be required. By studying the relative motion through the use of mean orbit elements, we are able to ignore the orbit period specific oscillations and address the secular drift directly. It is not possible to set the drift of each orbit to zero. However, instead we choose to set the difference in mean orbit element drifts to zero to avoid *relative secular growth.*

Numerous analytic theories for the motion of an artificial satellite have been developed. The one developed by Coffey and Deprit is the most comprehensive [4]; it has been developed to third order with zonals up to at least J_9. In this study we use the theory developed by Brouwer [2]. We want to look at the motion defined by the mean elements, thus we will use the averaged elements, or in Brouwer's notation, the double-primed elements. This is the Hamiltonian after removal of the short and long period terms. Since $J_n = \mathcal{O}(J_2^2)$ for $n > 2$, the only geopotential effect that is included is J_2.

The orbit geometry is described through the Delaunay orbit elements l (mean anomaly), g (argument of perigee) and h (longitude of the ascending node) with the associated generalized momenta L, G and H defined as

$$L = \sqrt{\mu a}, \tag{1a}$$

$$G = \sqrt{\mu a(1 - e^2)} = L\eta, \tag{1b}$$

$$H = G\cos i, \tag{1c}$$

where a is the semi-major axis, e is the eccentricity and i is the inclination angle. The variable η is another convenient parameter measuring the eccentricity and is defined as

$$\eta = \sqrt{1 - e^2}. \tag{2}$$

Note that G is the angular momentum of the orbit and H is the corresponding polar component. Unless noted otherwise, any orbit elements used from here on will be assumed to be mean orbit elements. Since the Delaunay variables are canonical variables, given the Hamiltonian M, their rates are found through the partial derivatives

$$\dot{l} = \frac{\partial M}{\partial L}, \qquad \dot{g} = \frac{\partial M}{\partial G}, \qquad \dot{h} = \frac{\partial M}{\partial H}, \tag{3a}$$

$$\dot{L} = -\frac{\partial M}{\partial l}, \qquad \dot{G} = -\frac{\partial M}{\partial g}, \qquad \dot{H} = -\frac{\partial M}{\partial h}. \tag{3b}$$

The mean Hamiltonian M can be written as an asymptotic expansion in $\epsilon = -J_2$ as

$$M = M_0 + \epsilon M_1 + \mathcal{O}(\epsilon^2). \tag{4}$$

In this study, we will only focus on the first order terms and ignore higher order terms in ϵ. The first two terms M_0 and M_1 are given by

$$M_0 = -\frac{\mu^2}{2L^2}, \tag{5}$$

$$M_1 = -\frac{\mu^4 R_e^2}{4L^6}\left(\frac{L}{G}\right)^3\left(1 - 3\frac{H^2}{G^2}\right), \tag{6}$$

with R_e being Earth's radius at the equator. The following algebra is greatly simplified if we work with dimensionless variables. Therefore distances will be measured in Earth radii R_e and time is normalized by the mean motion of a satellite at one Earth radius (i.e. $\mu = 1$). The dimensionless equivalents of Equations (5) and (6) are

$$M_0 = -\frac{1}{2L^2}, \tag{7}$$

$$M_1 = -\frac{1}{4L^6}\left(\frac{L}{G}\right)^3\left(1 - 3\frac{H^2}{G^2}\right). \tag{8}$$

The transformation between osculating and mean elements is shown in the appendix. Note that Brouwer's classical theory is known to have difficulties in translating mean elements into corresponding osculating elements for near-circular orbits and near-equatorial orbits. These problems can be overcome by applying the modifications to Brouwer's artificial satellite theory suggested by Lyddane [6] or by using Aksnes reformulation of Brouwer's theory [1]. However, the mean to osculating mapping problems are a practical issue which do not directly affect the analytical results developed in this paper. The J_2 invariant orbit constraints are not dependent on what theory is used to map between mean and osculating orbit elements.

Since both M_0 and M_1 depend solely on the mean momenta L, G and H (i.e. the angle variables are ignorable), according to Equation (3b) the mean momenta expressions are constant. Using Equation (3a), the mean angle rates $\dot{l}$, $\dot{g}$ and $\dot{h}$ are

$$\dot{l} = \frac{1}{L^3} + \epsilon\frac{3}{4L^7}\left(\frac{L}{G}\right)^3\left(1 - 3\frac{H^2}{G^2}\right) = \frac{1}{L^3} + \epsilon\frac{3}{4L^7\eta^3}\left(1 - 3\cos^2 i\right), \tag{9}$$

$$\dot{g} = \epsilon\frac{3}{4L^7}\left(\frac{L}{G}\right)^4\left(1 - 5\frac{H^2}{G^2}\right) = \epsilon\frac{3}{4L^7\eta^4}\left(1 - 5\cos^2 i\right), \tag{10}$$

$$\dot{h} = \epsilon\frac{3}{2L^7}\left(\frac{L}{G}\right)^4\left(\frac{H}{G}\right) = \epsilon\frac{3}{2L^7\eta^4}\cos i. \tag{11}$$

Since the mean momenta rates $\dot{L}$, $\dot{G}$ and $\dot{H}$ are always zero, we will only be concerned with matching the angle rates between two neighboring orbits in the

next section. For the following development L, η and i will be used as the primary momenta variables.

3. Constraints for J_2 Invariant Orbits

In order to prevent two neighboring orbits from drifting apart, the average secular growth needs to be equal. Short period oscillations can be ignored here since these are only 'temporary' deviations. The long period rates appear secular over a few weeks and they are $\mathcal{O}(J_2^2)$. Thus, they are of higher order than the terms we are considering.

Since the mean angle quantities l, g and h do not directly contribute to the secular growth caused by J_2, their values can be chosen at will. However, the mean momenta values L, G and H (and therefore implicitly a, e and i) must be carefully chosen to match the secular drift rates.

To keep the satellites from drifting apart over time, it would be desirable to match all three rates $(\dot{l}, \dot{g}, \dot{h})$. However, as will be shown, this can only be achieved by having the momenta equal, which severely restricts the possible relative orbits. Therefore, we impose the condition that the relative average drift rate of the angle between the radius vectors be zero. This results in

$$\dot{h}_i = \dot{h}_j, \qquad \forall i \neq j, \tag{12}$$

$$\dot{\theta}_i = \dot{l}_i + \dot{g}_i = \dot{\theta}_j, \qquad \forall i \neq j, \tag{13}$$

where θ is the mean argument of latitude. Thus, the perigees are able to drift apart. Combining Equations (9) and (10), the mean latitude rate $\dot{\theta}$ is expressed as

$$\dot{\theta} = \frac{1}{L^3} + \epsilon \frac{3}{4L^7\eta^4}[\eta(1 - 3\cos^2 i) + (1 - 5\cos^2 i)]. \tag{14}$$

Let the reference mean orbit elements be denoted with the subscript '0'. The drift rate $\dot{\theta}_i$ of a neighboring orbit can be written as a series expansion about the reference orbit element as

$$\dot{\theta}_i = \dot{\theta}_0 + \frac{\partial \dot{\theta}_0}{\partial L}\delta L + \frac{\partial \dot{\theta}_0}{\partial \eta}\delta\eta + \frac{\partial \dot{\theta}_0}{\partial i}\delta i + H.O.T., \tag{15}$$

where we make use of the fact that $\dot{\theta} = \dot{\theta}(L, \eta, i)$ only. Note that this theory will lead to an analytical first order condition on the mean orbit elements. To establish a more precise set of orbit elements satisfying Equations (12) and (13), either δL, $\delta\eta$ or δi could be chosen and the remaining two momenta orbit element differences found through a numerical root solving technique. However, the analytical first order conditions provide reasonably accurate solutions to these two constraints equations and provide a wealth of insight into the behavior of J_2 invariant relative orbits.

Let the difference in mean latitude rates be $\delta\dot{\theta}$, then a first order approximation of Equation (15) is written as

$$\delta\dot{\theta} = \dot{\theta}_i - \dot{\theta}_0 = M_{\theta L}\delta L + M_{\theta\eta}\delta\eta + M_{\theta i}\delta i, \tag{16}$$

where $M_\theta = M_l + M_g$ and

$$M_{\alpha A} = \left.\frac{\partial\dot{\alpha}}{\partial A}\right|_{L=L_0, G=G_0, H=H_0}. \tag{17}$$

Similarly, we can expand the nodal rate $\dot{h}$ to find

$$\delta\dot{h} = M_{hL}\delta L + M_{h\eta}\delta\eta + M_{hi}\delta i. \tag{18}$$

To enforce equal drift rates $\dot{\theta}_i$ and $\dot{h}_i$ between neighboring orbits, we must set $\delta\dot{\theta}$ and $\delta\dot{h}$ equal to zero in Equations (16) and (18), resulting in the following two necessary conditions for relative orbits to be J_2 invariant up to first order

$$M_{\theta L}\delta L + M_{\theta\eta}\delta\eta + M_{\theta i}\delta i = 0, \tag{19}$$

$$M_{hL}\delta L + M_{h\eta}\delta\eta + M_{hi}\delta i = 0. \tag{20}$$

Since Equations (19) and (20) have three unknown quantities, namely the differences in mean momenta elements δL, $\delta\eta$ and δi, we are only left with one degree of freedom in selecting the relative momenta. After choosing either δL, $\delta\eta$ or δi, the remaining two momenta differences are determined through the two conditions shown above. If we choose to enforce that the various $\dot{l}_i$ and $\dot{g}_i$ are equal, then we have a nonlinear system of three variables with three constraints, leaving no degree of freedom in choosing the momenta quantities L, η and i. These conditions are only satisfied for particular orbit solutions which are of little interest for spacecraft formation flying.

Since the mean anomaly, argument of perigee and right ascension are ignorable coordinates in the mean element space, they have no effect on the secular rates between two objects. In the osculating space they are not ignorable and consequently have an effect on the secular relative motion. The angle differences δl, δg and δh can therefore be chosen at will. Thus, operating in mean element space has reduced the scope of the problem. This leaves us with a total of four degrees of freedom to design a J_2 invariant relative orbit. In contrast, with $J_2 = 0$, there is only the constraint $\delta a = 0$ leaving us five degrees of freedom.

Taking the partial derivartives of Equations (9) and (10), we are able to rewrite the condition in Equation (19) which enforces equal mean latitude rates.

$$\begin{aligned}
&-\frac{3}{{L_0}^4}\delta L - \epsilon\frac{21}{4L_0^8\eta_0^4}[\eta_0(1-3\cos^2 i_0) + (1-5\cos^2 i_0)]\delta L - \\
&\quad -\epsilon\frac{3}{4L_0^7\eta_0^5}[3\eta_0(1-3\cos^2 i_0) + 4(1-5\cos^2 i_0)]\delta\eta + \\
&\quad +\epsilon\frac{3}{2L_0^7\eta_0^4}(3\eta_0+5)\cos i_0 \sin i_0\delta i = 0.
\end{aligned} \tag{21}$$

Note that only the term δL appears without being multiplied by the small parameter ϵ. Thus δL must be itself of $\mathcal{O}(\epsilon)$ and the term involving $\epsilon\delta L$ can be dropped as a higher order term. The first necessary condition is then simplified to

$$-\delta L - \epsilon\frac{1}{4L_0^3\eta_0^5}[3\eta_0(1-3\cos^2 i_0)+4(1-5\cos^2 i_0)]\delta\eta + \\ +\epsilon\frac{1}{2L_0^3\eta_0^4}(3\eta_0+5)\cos i_0 \sin i_0 \delta i = 0. \tag{22}$$

Taking the partial derivatives of Equation (11), we are able to rewrite the second condition for J_2 invariant orbits, given in Equation (20), as

$$\epsilon\frac{3}{2L_0^7\eta_0^5}\left[-\frac{7}{L_0}\cos i_0\delta L - 4\cos i_0\delta\eta - \eta_0 \sin i_0\delta i\right] = 0. \tag{23}$$

Since $\delta L = \mathcal{O}(\epsilon)$ the δL term is dropped, resulting in the simplified necessary condition

$$\delta\eta = -\frac{\eta_0}{4}\tan i_0\delta i, \tag{24}$$

which enforces equal nodal rates $\dot{h}$. Note that as the master orbit inclination angle approaches 90 degrees, the change in eccentricity necessary to compensate for an inclination angle difference grows infinitely large. Using the δi defined in Equation (24), we are able to simplify the condition in Equation (22) to

$$\delta L = \underbrace{-\frac{\epsilon}{4L_0^4\eta_0^5}(4+3\eta_0)(1+5\cos^2 i_0)}_{D} L_0\delta\eta. \tag{25}$$

Combined, Equations (24) and (25) provide the two necessary conditions on the mean momenta differences between two neighboring orbits to yield a J_2 invariant relative orbit.

For more physical insight into these constraints, it is convenient to map the differences in L into differences in the semi-major axis a. The reason for choosing to deal with variations in η and not the eccentricity measure e itself will become clear shortly. Recalling that $L = \sqrt{a}$ (L is a non-dimensional variable), the variations in L and a are related through

$$\delta L = \frac{1}{2L}\delta a = \frac{\delta a}{2\sqrt{a}}. \tag{26}$$

Substituting Equations (26) into Equation (25), the constraint enforcing equal mean latitude rates between two orbits is rewritten as

$$\delta a = 2Da_0\delta\eta. \tag{27}$$

Note that this a is the non-dimensional semi-major axis and must be multiplied by the Earth radius R_e to obtain proper physical units. Combined, Equations (24) and

(27) form the two necessary momenta constraints expressed in terms of a difference in semi-major axis, eccentricity and inclination angle. Please note that these constraint conditions are not justified near the critical inclination angle. A different orbit theory would need to be used to research this situation further.

To write the constraint in Equation (24) in terms of the eccentricity e directly, we must take the first variation of $\eta = \sqrt{1 - e^2}$.

$$\delta e = -\frac{\eta}{e}\delta\eta. \tag{28}$$

Substituting this into Equation (24) we find

$$\delta e = \frac{(1 - e^2)\tan i}{4e}\delta i. \tag{29}$$

Clearly numerical difficulties arise with this constraint expression whenever $e \to 0$ and the reference orbit becomes circular. According to Equation (29), it would appear that the change in eccentricity required for a given δi would grow infinitely large as e becomes zero. However, Equation(24) shows that this is not necessary. Using η as the eccentricity measure, we find that the change in eccentricity reaches a finite limit for a circular orbit. The reason for this discrepancy is that it is not the constraint condition that causes the singularity, but the transformation between variations in e and η in Equation (28). To avoid numerical difficulties with circular reference orbits when setting up necessary mean orbit element differences, it is therefore convenient to describe necessary changes in eccentricity through $\delta\eta$ and then use the nonlinear mapping $e = \sqrt{1 - \eta^2}$ to compute the adjusted eccentricity.

If J_2 is set to zero (i.e. pure Keplerian motion), then we are only left with the constraint that $\delta a = 0$. This makes sense intuitively, since the semi-major axis a determines the orbit period. For Keplerian motion, if the orbit periods are not equal, then the two spacecraft will drift apart. In the momenta space (a, e, i) this constraint represents the surface of a sphere as illustrated in Figure 1. For a particular chief orbit with a_0, e_0 and i_0, the neighboring orbit momenta elements must lie on this surface. However, once the J_2 perturbation is included, the geometric constraint on the momenta elements to achieve drift free relative motion is a straight line which is not tangent to the sphere surface.

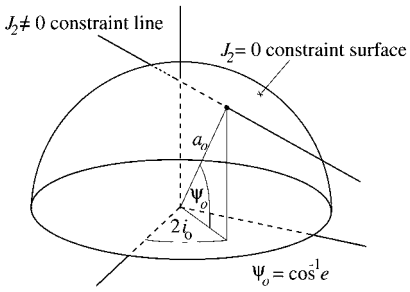

Figure 1. Drift free constraint illustration in momenta space.

It is interesting to study the energy levels of two neighboring orbits which are J_2 invariant using the necessary first order conditions established in Equations (24) and (27). For the system studied, the Hamiltonian M is the total energy. Including the J_2 term, the averaged energy in terms of normalized orbit elements is given by

$$M = -\frac{1}{2a} + \epsilon \frac{1}{4a^3\eta^3}(-1 + 3\cos^2 i). \tag{30}$$

Where for Keplerian motion the energy level of an orbit only depends on the semi-major axis a, including the J_2 effect makes the energy expression depend on all three momenta elements a, e and i. The difference in energy δM of a neighboring orbit and a reference orbit is approximated as

$$\delta M = M - M_0 \approx \frac{\partial M_0}{\partial a}\delta a + \frac{\partial M_0}{\partial \eta}\delta\eta + \frac{\partial M_0}{\partial i}\delta i. \tag{31}$$

Computing the partial derivatives in Equation (30) while keeping in mind that δa is of order $\mathcal{O}(\epsilon)$ we find that

$$\delta M = \frac{1}{2a_0^2}\delta a + \epsilon \frac{3}{4a_0^3\eta_0^4}[(1 - 3\cos^2 i_0)\delta\eta - 2\eta_0 \sin i_0 \cos i_0 \delta i]. \tag{32}$$

For two neighboring orbits to be J_2 invariant, the differences in a, η and i must abide the two conditions in Equations (24) and (27). Substituting these variational constraint, the energy difference between two J_2 invariant orbits is given by

$$\delta M = \epsilon \frac{\tan i_0}{4a_0^3\eta_0^4}(1 + 5\cos^2 i_0)\delta i. \tag{33}$$

Equation (33) states that if the two orbits have a non-zero difference in inclination angle δi (or implicitly a difference in η or a), then the two orbits must have different energies. Only if all three momenta elements a, η and i between two orbits are equal will the orbit energies themselves be equal. Note that this condition still allows the two orbits to have different mean l, g and h.

Note that Equation (24) shows a fundamental limitation of these mean momenta constraints. For near-polar orbits, where the inclination angle is close to 90 degrees, the $\tan i$ term grows very large. Even a small change in inclination angle δi, typically done to achieve out-of-plane relative motion in polar regions, would result in a relatively large change in eccentricity. The result is that the resulting J_2 invariant relative orbits grow very large for near-polar orbits, making these orbits of little practical use for close formation flying applications. An analogous conclusion is made studying the relative energy condition in Equation (33). Since the relative orbit energy difference grows infinitely large for a polar orbit, it is clear that for near-polar reference orbits the J_2 invariant relative orbit would be very large. However, note that the three mean angle variables l, g and h can still be picked at random without causing any orbit drift, even for the polar case. Further, note that if

a change in eccentricity is prescribed for a near-polar orbit, the associated required change in inclination angle would be very small. Thus enforcing equal drift rate conditions for near-polar orbits only encounter practical difficulties if a particular change in orbit inclination angle is demanded. As numerical simulations will show, setting up this worst case problem in mean element space and then transforming to corresponding inertial position and velocity vectors will typically still exhibit less secular drift than if the problem is simply setup using osculating elements. Further, while it will not be possible to perfectly compensate for the ascending node drift difference due to δi, it is still possible to equalize the mean latitude rate drifts $\dot{\theta}_i$ using Equation (27).

4. Numerical Simulations

Two numerical studies are presented illustrating J_2 invariant relative orbits for both non-polar and near-polar master orbits. The orbit elements for the master orbit are the same for each simulation except for the inclination angle i as shown in Table I. The orbit has an altitude of 775 km. The parameter J_2 is 0.0001082 and the Earth's radius is set at 6378.1363 km. Since each spacecraft is assumed to be of equal type, differential drag effects are ignored here. The purpose of these simulations is to illustrate how well the first order conditions in Equations (24) and (27) render the resulting relative orbit J_2 invariant. Further, the power of setting up relative orbits in terms of mean orbit elements versus osculating element space is shown.

The relative orbit is constructed in these simulations by choosing particular differences in mean orbit elements, and then translating the adjusted mean orbit elements of the second satellite into corresponding osculating orbit elements. The numerical simulation then uses the corresponding initial position and velocity vector and solves the system using the nonlinear equations of motion including the

TABLE I
Master satellite orbit eements.

Desired average orbit elements	Value	Units
a	7153	km
e	0.05	
i	48 or 88	degree
h	0.0	degree
g	30.0	degree
l	0.0	degree

zonal J_i terms up to fifth order. However, in all cases tested the inclusion of the J_3 through J_5 terms had a minimal effect on the answer.

Other techniques could be used as well to setup the initial relative orbit. For example, it is possible to establish a desired relative orbit using the natural solutions of the linear CW equations. Since this is the desired mean behavior, these six position and velocity coordinates must then be first translated into six corresponding mean orbit elements. Thus we are able to make use of the analytic first order transformation shown in the appendix to obtain the corresponding initial osculating elements (i.e. actual position and velocity vector).

4.1. NON-POLAR MASTER ORBIT

The first simulation illustrates how well the matching conditions work for non-polar orbits. Here the inclination angle is set to 48 degrees. The relative orbit is described by choosing the following mean orbit element differences. To achieve some out-of-plane motion, an ascending node difference of $\delta h = 0.005$ degrees is prescribed. The line of perigee and initial mean anomaly differences are set equal and opposite in sign as $\delta g = 0.01$ degrees and $\delta l = -0.01$ degrees. Of the three momenta elements, we chose to prescribe a change in eccentricity $\delta e = 0.0001$ to exaggerate the in-plane, relative orbit. Using Equations (24) and (27), the corresponding changes in a and i must be $\delta a = -0.351765$ m and $\delta i = 0.001035$ degrees. Note that both the required δa and δi to compensate for this δe are rather small.

The resulting relative orbits, as seen in the Local-Vertical–Local-Horizontal (LVLH) frame, are shown in Figure 2. The rotating LVLH frame is defined with its first axis being along the chief orbit radial axis, the third is along the orbit normal

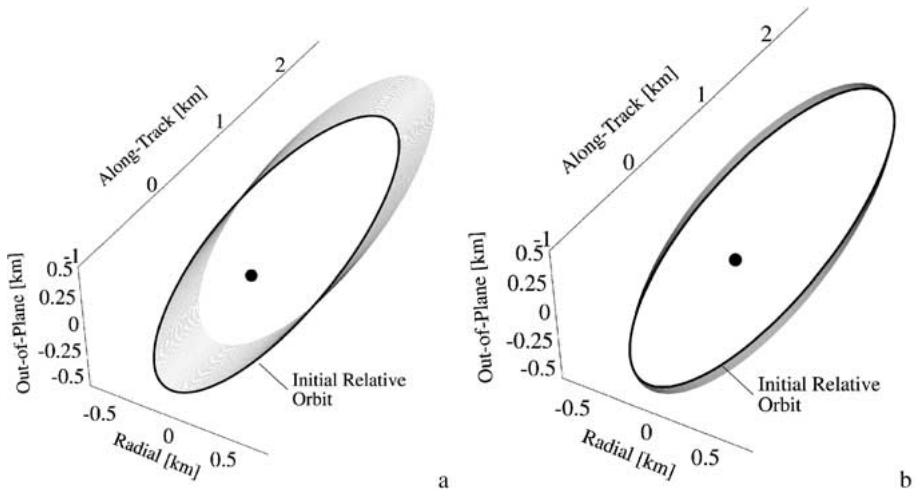

Figure 2. (a) Initial relative orbit setup in osculating elements. (b) Initial relative orbit setup in mean elements.

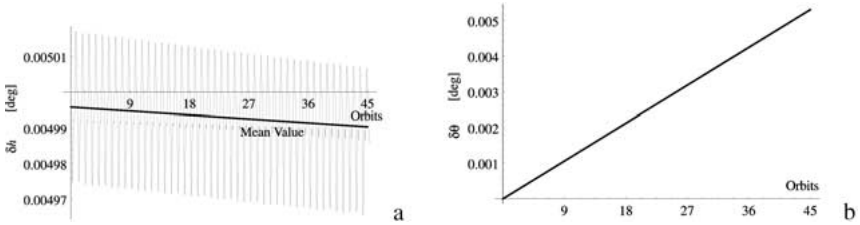

Figure 3. (a) Difference in ascending node h for osculating element setup. (b) Difference in mean latitude angle θ for osculating element setup.

direction, and the second being orthogonal to the previous two satisfying the right-hand rule. The plots always show the data of 45 orbits, which correspond to roughly 3 days of simulation time. The LVLH frame is chosen such that the $\hat{x}$ direction is along the instantaneous master satellite position vector. The out-of-plane component $\hat{z}$ is found by computing the cross product of $\hat{x}$ with the normalized velocity vector. The along track $\hat{y}$ direction is then found by taking the cross product of $\hat{z}$ and $\hat{x}$. The initial relative orbit is always shown as a solid black line, while the path of the remaining 45 orbits is shown as a gray line. Both simulations use the same initial orbit element differences. In Figure 2(a) the initial orbit element differences, which determine the initial shape of the relative orbit, are chosen in osculating element space. Substantial relative orbit drift is apparent due to the perturbative influence of J_2. Figure 2(b) illustrates the drastic improvements that may occur if the initial orbit geometry is setup in mean element space. Since the matching conditions in Equation (24) and (27) are only up to first order, the relative orbit will not necessarily be perfectly J_2 invariant. While some periodic thrusting is still necessary, the frequency of these orbit corrections can be greatly reduced.

The differences of δh and $\delta\theta$ between the master and secondary orbits are shown in Figure 3 for the case where the initial setup is performed in the osculating element space. The mean orbit elements are shown as a solid black line, while the osculating elements are shown as a gray line. The corresponding orbit element differences are shown in Figure 4 for the case where the setup is performed in mean element space. While for an inclination angle of 48 degrees both orbits experience a substantial nodal rate $\dot{h}$, the difference in ascending node rates is rather small. Setting up the relative geometry in mean element space does reduce the relative

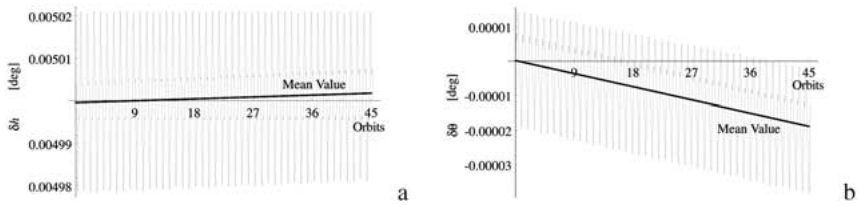

Figure 4. (a) Difference in ascending node h for mean element setup. (b) Difference in mean latitude angle θ for mean element setup.

nodal drift, but not substantially. A rough calculation of the Δv required per year to compensate for this drift shows 0.0725 m/s required for the osculating element setup, and only 0.0181 m/s required for the mean element setup. Both are relatively small numbers. At this inclination, the $\dot{\theta}$ drift is the dominant factor pulling the two orbits apart. Comparing Figures 3(b) and 4(b) the benefit of using mean elements is clear. Using the osculating setup where the initial chief and deputy orbit elements are constructed in osculating orbit element, the Δv required per year is roughly 40.15 m/s. Using the mean orbit elements to setup the geometry reduces this to 0.145 m/s. Using the momenta element matching condition and working in mean orbit element space, we are able to substantially reduce the J_2 induced drift and the corresponding Δv's required to reset the relative orbits.

4.2. NEAR-POLAR MASTER ORBIT

The second simulation illustrates some issues that arise when trying to generate J_2 invariant relative orbits for near-polar master orbits and demanding a specific inclination angle difference for out-of-plane motion. The inclination angle is set to 88 degrees for this purpose. The relative orbit is described by choosing the mean orbit element differences $\delta h = 0.0$ degrees (all out-of-plane motion produced through δi), $\delta g = 0.1$ degrees and $\delta l = -0.1$ degrees. Assume the relative orbit geometry requires a δi of 0.01 degrees to achieve roughly 1 km of out-of-plane motion. However, we are no longer able to use both matching conditions in Equations (27) and (24) since the $\tan i$ term will result in impractical large changes in eccentricity. Therefore, we abandon the hope to be able to compensate for the δh drifts. For near polar orbits, even though the various $\dot{h}$ rates are relatively small, the differences of these rates between neighboring orbits with different inclination angles are large. However, we are still able to use Equation (27) to match mean latitude drift rates. Therefore we are left with one unused degree of freedom and choose a δe of 0.0001 to exaggerate the in-plane relative orbit.

As the illustrations in Figures 5 and 6 show, the J_2 induced drift can still be reduced by simply setting up the relative geometry in mean element space. Figure 5(a) illustrates the motion resulting from setting up the desired orbit element differences in osculating orbit space. The relative orbits pull apart substantially in three days. Figure 5(b) shows the reduced amount of drift that occurs if the same orbit element differences are setup in mean element space. Note that Equation (27) has not been utilized here to compensate for the mean latitude difference drift. The relative orbit is thus seen to drift in the negative along track direction. In Figure 6(a) the semi-major axis a is adjusted using Equation (27) to attempt to equalize the mean latitude rates $\dot{\theta}$. The required δa is -0.24157 m. While there is still some drift in the relative orbits due to the different $\dot{h}$ rates, the orbits no longer pull apart due to different mean latitude rates. Figure 6(b) shows how the relative orbit may become excessively large if we attempt to cancel all relative orbit drift for near-polar orbits. To achieve a desired δi of 0.01 degrees, the other two momenta

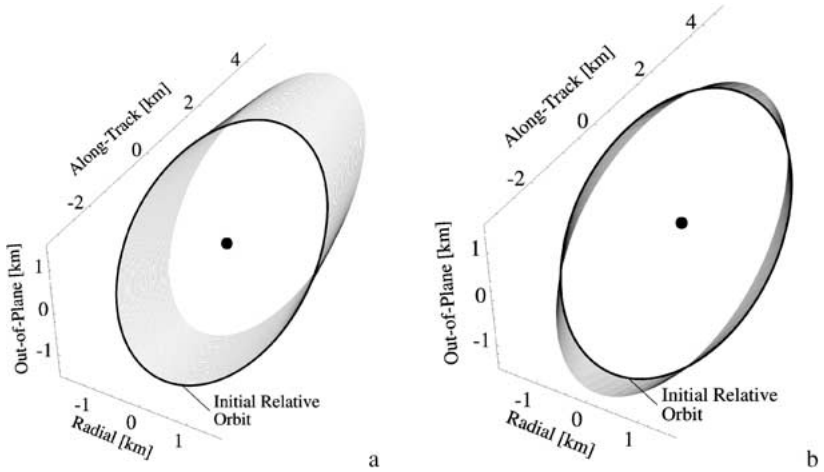

Figure 5. (a) Initial relative orbit setup in osculating elements. (b) Initial relative orbit setup in mean elements.

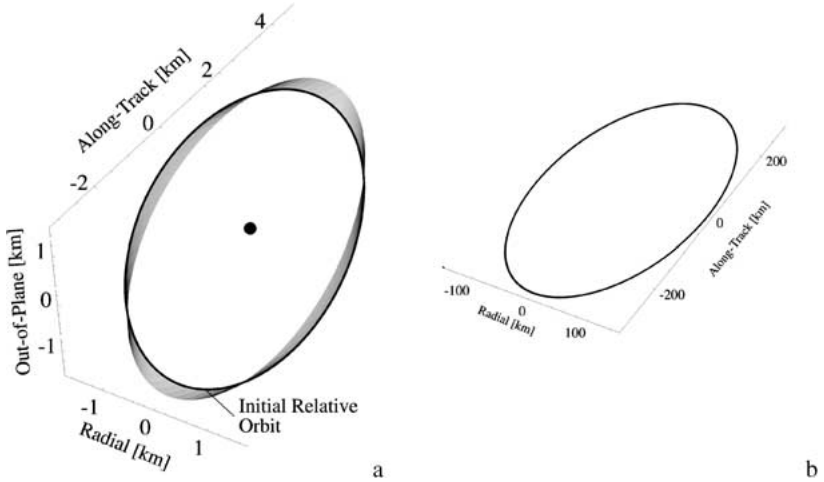

Figure 6. (a) Initial relative orbit setup in mean elements using $\delta a = 2Da\delta\eta$. (b) Initial relative orbit setup in mean elements using both matching conditions.

elements differences must be $\delta e = 0.020648$ and $\delta a = -27.2122$ m. While the resulting near-polar relative orbit has essentially no drift as seen in this scale, the relative orbit radius grows from a few kilometers to over 100 km. Note that the desired ± 1 km out-of-plane motion isn't even visible on the scale shown.

The differences in ascending node and mean latitude angles for the cases where the relative orbit geometry is setup in the osculating space and where it is setup in the mean element space with semi-major axis adjustment are shown in Figures 7 and 8. As predicted, the ascending node drift δh is the same for both cases since

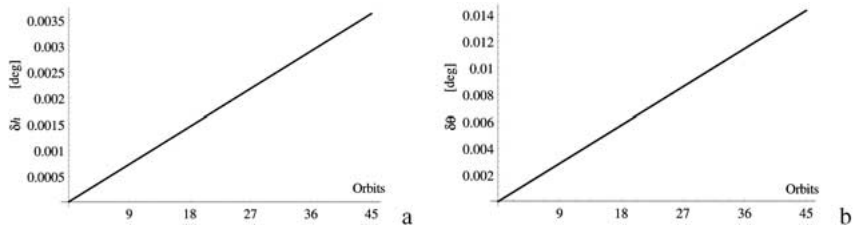

Figure 7. (a) Difference in ascending node h for osculating element space setup for a near-polar master orbit. (b) Difference in mean latitude angle θ for osculating element space setup for a near-polar master orbit.

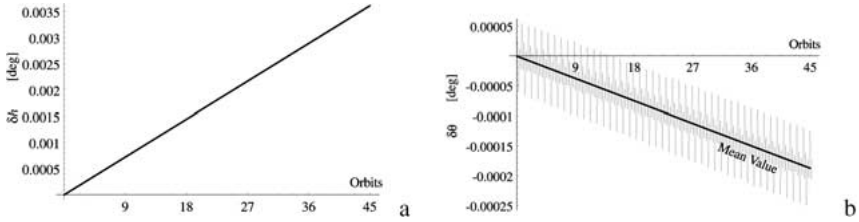

Figure 8. (a) Difference in ascending node h for mean element space setup for a near-polar master orbit. (b) Difference in mean latitude angle θ for mean element space setup for a near-polar master orbit.

we are no longer trying to compensate for this. Over a year, the Δv required to compensate for this drift is roughly 56.8 m/s. However, where the osculating element setup results in a substantial mean latitude drift $\delta\theta$, setting up the orbits in mean element space and compensating through a corresponding δa results in a substantially reduced mean latitude drift. The Δv requirement to compensate for the $\delta\theta$ is approximately 112 m/s for the osculating setup. This Δv drops to 14.1 m/s if the orbit elements are setup in mean element space. The Δv requirement per year is then further reduced to approximately 1.45 m/s if the δa adjustment is made to equalize the averaged mean latitude rates.

While this method is not able to compensate for the δh drift encountered with near-polar orbits, it is possible to establish an approximate solution that greatly reduces the J_2 induced relative orbit drift. Note that prescribing differences to h, g and l is always possible, even for polar master orbits. Problems may arise when trying to match a, e and i for a prescribed difference in one of the quantities.

5. Conclusion

A method is presented to establish J_2 invariant relative orbits for spacecraft formation flying applications. The desired relative orbit geometry is designed using differences in mean orbit elements. Two constraints on the three momenta element differences δa, δe and δi are derived. These leave a total of four degrees of freedom

to design the relative orbit. As the inclination angle i approaches a polar orbit, the corrections required in eccentricity and semi-major axis to compensate for the J_2 effect become too large to be of practical value. Working with near-polar orbits, setting up the relative orbit geometry in mean elements and canceling the mean latitude rate difference still provides a substantial drift and associated fuel savings. A particular limitation of the presented method is that the mapping between mean and osculating elements goes singular for circular orbits. The momenta element differences constraints still hold for circular orbits, but the mapping from mean to osculating elements has mathematical problems whenever e approaches zero. This can be rectified by using non-singular elements.

Acknowledgements

This research was supported by the Air Force Office of Scientific Research under Grant F49620-99-1-0075.

Appendix

For completeness, this appendix illustrates the transformation between osculating and mean orbit elements. This is accomplished through two transformations. The first transformation maps osculating elements to intermediate or long period elements, while the second transformation maps long period elements to mean elements. Using Brouwer's notation, the long period elements are denoted with a single prime, while the mean elements are denoted with a double prime. The generating function $W_1^{\rm sp}$, which establishes the osculating to long period elements transformation, is given in terms of non-dimensional Delaunay variables as

$$W_1^{\rm sp} = \frac{1}{4G^3}\Bigg(\left(-1+3\frac{H^2}{G^2}\right)(f-l+e\sin f)+\frac{3}{2}\left(1-\frac{H^2}{G^2}\right)\times \\ \times\left(\sin(2f+2g)+e\sin(f+2g)+\frac{e}{3}\sin(3f+2g)\right)\Bigg). \tag{34}$$

The notation $W_1^{\rm sp}$ says that this is a first order transformation which removes the short period (sp) component. Coffey [4] accomplishes this with two transformations. The generating function $W_1^{\rm lp}$, which establishes the long period to mean elements transformation, is given by

$$W_1^{\rm lp} = -\frac{1}{32G^3}\left(1-\frac{G^2}{L^2}\right)\left(1-5\frac{H^2}{G^2}\right)^{-1}\left(1-16\frac{H^2}{G^2}+15\frac{H^4}{G^4}\right)\sin 2g. \tag{35}$$

The transformation between long period and osculating elements is achieved through

$$L' = L - \epsilon(L, W_1^{\rm sp}) = L + \epsilon \frac{\partial W_1^{\rm sp}}{\partial l}, \tag{36}$$

$$l' = l - \epsilon(l, W_1^{\rm sp}) = l - \epsilon \frac{\partial W_1^{\rm sp}}{\partial L} \tag{37}$$

with analogous transformations for the other momenta and angle orbit elements. The expression $(L, W_1^{\rm sp})$ is the Poisson bracket of L and $W_1^{\rm sp}$. The inverse for this transformation is achieved trivially by switching the primed and unprimed letters and reversing the sign of the ϵ term.

$$L = L' + \epsilon(L', W_1^{\rm sp}) = L - \epsilon \frac{\partial W_1^{\rm sp}}{\partial l'}, \tag{38}$$

$$l = l' + \epsilon(l', W_1^{\rm sp}) = l + \epsilon \frac{\partial W_1^{\rm sp}}{\partial L'}. \tag{39}$$

The long period to osculating elements transformations are then given by

$$\begin{aligned} L \;=\; & L' - \frac{\epsilon}{4L'^3}\left[\left(-1 + 3\frac{H'^2}{G'^2}\right)\left(\frac{a'^3}{r'^3} - \frac{L'^3}{G'^3}\right) + \right. \\ & \left. +\; 3\left(1 - \frac{H'^2}{G'^2}\right)\left(\frac{a'}{r'}\right)^3 \cos(2f' + 2g')\right], \end{aligned} \tag{40a}$$

$$\begin{aligned} G \;=\; & G' - \frac{3\epsilon}{4G'^3}\left(1 - \frac{H'^2}{G'^2}\right)\left[\cos(2f' + 2g') + \right. \\ & \left. +\; e'\cos(f' + 2g') + \frac{e'}{3}\cos(3f' + 2g')\right], \end{aligned} \tag{40b}$$

$$H = H', \tag{40c}$$

$$\begin{aligned} l \;=\; & l' + \frac{\epsilon}{8e'L'^4}\left(\frac{L'}{G'}\right)\left[2\left(-1 + 3\frac{H'^2}{G'^2}\right)\left(\frac{a'^2}{r'^2}\frac{G'^2}{L'^2} + \frac{a'}{r'} + 1\right)\sin f' + \right. \\ & +3\left(1 - \frac{H'^2}{G'^2}\right)\left(\left(-\frac{a'^2}{r'^2}\frac{G'^2}{L'^2} - \frac{a'}{r'} + 1\right)\sin(f' + 2g') + \right. \\ & \left. \left. +\; \left(\frac{a'^2}{r'^2}\frac{G'^2}{L'^2} + \frac{a'}{r'} + \frac{1}{3}\right)\sin(3f' + 2g')\right)\right], \end{aligned} \tag{40d}$$

$$
\begin{aligned}
g \;=\; & g' - \frac{\epsilon}{8e'L'^4}\left(\frac{L'}{G'}\right)^2\left[2\left(-1+3\frac{H'^2}{G'^2}\right)\left(\frac{a'^2}{r'^2}\frac{G'^2}{L'^2}+\frac{a'}{r'}+1\right)\sin f' + \right. \\
& +3\left(1-\frac{H'^2}{G'^2}\right)\left(\left(-\frac{a'^2}{r'^2}\frac{G'^2}{L'^2}-\frac{a'}{r'}+1\right)\sin(f'+2g')+\right. \\
& \left.\left. + \left(\frac{a'^2}{r'^2}\frac{G'^2}{L'^2}+\frac{a'}{r'}+\frac{1}{3}\right)\sin(3f'+2g')\right)\right] - \\
& -\frac{3\epsilon}{8G'^4}\left[2\left(-1+5\frac{H'^2}{G'^2}\right)(f'-l'+e'\sin f')+\left(3-5\frac{H'^2}{G'^2}\right)\times\right. \\
& \left.\times\left(\sin(2f'+2g')+e'\sin(f'+2g')+\frac{e'}{3}\sin(3f'+2g')\right)\right], \qquad \text{(40e)}
\end{aligned}
$$

$$
\begin{aligned}
h \;=\; & h' + \frac{3\epsilon}{4G'^4}\frac{H'}{G'}\left(2(f'-l'+e'\sin f') - \sin(2f'+2g') - \right. \\
& \left. - \; e'\sin(f'+2g') - \frac{e'}{3}\sin(3f'+2g')\right). \qquad \text{(40f)}
\end{aligned}
$$

The transformation between long period to mean elements is achieved in a similar manner. For the (L', l') elements, they are given by

$$
L' = L'' + \epsilon(L'', W_1^{\mathrm{lp}}) = L'' - \epsilon\frac{\partial W_1^{\mathrm{lp}}}{l''}, \qquad \text{(41)}
$$

$$
l' = l'' + \epsilon(l'', W_1^{\mathrm{lp}}) = l'' + \epsilon\frac{\partial W_1^{\mathrm{lp}}}{L''} \qquad \text{(42)}
$$

with the remaining transformations generated in an analogous manner. The inverse transformation is again achieved by simply switching the prime's and double-prime's and reversing the sign of the ϵ term. The transformation from mean to long period elements is given by

$$
L' \;=\; L'' \qquad \text{(43a)}
$$

$$
\begin{aligned}
G' \;=\; & G'' + \frac{\epsilon}{16G''^3}\left(1-\frac{G''^2}{L''^2}\right)\left(1-16\frac{H''^2}{G''^2}+15\frac{H''^4}{G''^4}\right)\times \\
& \times\left(1-5\frac{H''^2}{G''^2}\right)^{-1}\cos 2g'', \qquad \text{(43b)}
\end{aligned}
$$

$$
H' \;=\; H'', \qquad \text{(43c)}
$$

$$l' = l'' - \frac{\epsilon}{16G''^4}\left(\frac{G''^3}{L''^3}\right)\left(1 - 16\frac{H''^2}{G''^2} + 15\frac{H''^4}{G''^4}\right) \times \times \left(1 - 5\frac{H''^2}{G''^2}\right)^{-1} \sin 2g'', \tag{43d}$$

$$g' = g'' + \frac{\epsilon}{32G''^4}\left(1 - 5\frac{H''^2}{G''^2}\right)^{-1}\left[\left(3 - \frac{G''^2}{L''^2}\right) \times \times \left(1 - 16\frac{H''^2}{G''^2} + 15\frac{H''^4}{G''^4}\right) - 2\frac{H''^2}{G''^2}\left(1 - \frac{G''^2}{L''^2}\right) \times \times \left(11 + 25\frac{H''^2}{G''^2} + 200\frac{H''^4}{G''^4}\left(1 - 5\frac{H''^2}{G''^2}\right)^{-1}\right)\right] \sin 2g'', \tag{43e}$$

$$h' = h'' + \frac{\epsilon}{16G''^4}\left(\frac{H''}{G''}\right)\left(1 - \frac{G''^2}{L''^2}\right)\left(1 - 5\frac{H''^2}{G''^2}\right)^{-1} \times \times \left(11 + 25\frac{H''^2}{G''^2} + 200\frac{H''^4}{G''^4}\left(1 - 5\frac{H''^2}{G''^2}\right)^{-1}\right) \sin 2g'' \tag{43f}$$

References

1. Aksnes, K.: 1972, 'On the use of the hill variables in artifical satellite theory: Brouwer's theory', *J. Astr. Astrophy.* **17**, 70–75.
2. Brouwer, D.: 1959, 'Solution of the problem of artifical satellite theory without drag'. *Astronaut. J.* **64**(1274), 378–397.
3. Carter, T. E.: 1998, 'State transition matrix for terminal rendezvous studies: Brief survey and new example'. *J. Guid. Nav. Cont.* 148–155.
4. Coffey, S. L. and Deprit, A.: 1982, 'Third order solution for artificial satellites'. *AIAA J. Guid. Cont. Dyn.* **5**(4).
5. Kapila, V., Sparks, A. G., Buffington, J. M. and Yan, Q.: 1999, 'Spacecraft Formation Flying: Dynamics and Control', In: *Proceedings of the American Control Conference*, San Diego, California, pp. 4137–4141.
6. Lyddane, R. H.: 1963, 'Small eccentricities or inclinations in the Brouwer theory of the artificial satellite', *Astronom. J.* **68**(8), 555–558.
7. Sedwick, R., Miller, D. and Kong, E.: 1999, 'Mitigation of Differential Perturbations in Clusters of Formation Flying Satellites', In: *AAS/AIAA Space Flight Mechanics Meeting*. Paper No. AAS 99–124.
8. Xing, G. Q., Parvez, S. A. and Folta, D.: 1991, 'Implementation of Autonomous GPS Guidance and Control for the Spacecraft Formation Flying', In: *Proceedings of the American Control Conference*. San Diego, California, pp. 4163–4167.